A comprehensive thermo-viscoelastic experimental investigation of Ecoflex polymer

Zisheng Liao, Mokarram Hossain, Xiaohu Yao, Rukshan Navaratne, Grégory Chagnon

A comprehensive thermo-viscoelastic experimental investigation of Ecoflex polymer

Zisheng Liao[a,b], Mokarram Hossain[b,*], Xiaohu Yao[a,c,*], Rukshan Navaratne[d], Gregory Chagnon[e]

[a]*School of Civil Engineering and Transportation, South China University of Technology, 510640 Guangzhou, Guangdong, China*
[b]*Zienkiewicz Centre for Computational Engineering, College of Engineering, Swansea University, SA1 8EN, United Kingdom*
[c]*State Key Laboratory of Subtropical Building Science, South China University of Technology, 510640 Guangzhou, China*
[d]*Aerospace Engineering Department, University of South Wales, Pontypridd, Cardiff, United Kingdom*
[e]*University of Grenoble Alpes, CNRS, Grenoble INP, TIMC-IMAG, F-38000 Grenoble, France*

Abstract

Silicone polymers have enormous applications, especially in the areas of biomedical engineering. Ecoflex, a commercially available room temperature cured silicone polymer, has attracted considerable attention due to its wide range of applications as medical-grade silicones and as matrix materials in producing nano-filled stretchable sensors and dielectric elastomers for soft robotics. In this contribution, we have conducted a wide range of experiments under thermo-mechanical loadings. These experiments consist of loading-unloading cyclic tests, single-step relaxation tests, Mullins effects tests at different strain rates and stretches, stress recovery tests at different rest time etc. In order to assess the temperature influences on Ecoflex, a number of viscoelastic tests are performed in a thermal chamber with temperature ranging from -40°C to 140°C. Extensive experimental findings illustrate that Ecoflex experiences a significant stress softening in the first cycles and such a softening recovers gradually with respect to time. It also shows a significant amount of cyclic dissipation at various stretch levels as well as a considerable stress relaxation only for virgin samples. Cyclic dissipations and stress relaxation almost disappear for the case of pre-stretched samples. Furthermore, the material is more or less sensitive under a wide range of temperature differences.

Keywords: Ecoflex silicone rubber, Mullins effect, Stress recovery, Strain rate dependence, Temperature dependence

1. Introduction

Many silicone polymers have promising properties, such as bio-compatibility, good transparency, non-toxicity, good dielectric properties, high hydrophobicity, thermal stability, good processability, climate, oxidative, and UV resistances. Another aspect of silicones is that they do not react with most chemicals. Good bio-compatibility and relatively inert actions with chemicals make them one of the crucial engineering materials especially in biomedical applications, e.g., for tubing, peristaltic pumps, catheters and cardiovascular devices such as heart pumps, ventricular assist devices, cannulas and vascular grafts [1]. Furthermore, RTV (Room Temperature Vulcanisation) silicones have been used for skin-like applications or external maxillofacial prosthetics [2]. As their stiffness values match those attributed to compliant biological tissues, silicone

*Corresponding authors
Email addresses: l.zisheng@mail.scut.edu.cn (Zisheng Liao), mokarram.hossain@swansea.ac.uk (Mokarram Hossain), yaoxh@scut.edu.cn (Xiaohu Yao), rukshan.navaratne@southwales.ac.uk (Rukshan Navaratne), gregory.chagnon@univ-grenoble-alpes.fr (Gregory Chagnon)

polymers are massively used as substrates in mechanobiology. In addition to processability, transparency and non-toxicity, the possibility of relatively easy tuning of the mechanical properties of silicones by changing the polymer to curing agent ratio, or curing conditions is an attractive feature. These properties offer further advantages which favour the application of silicone-based elastomers in dynamic bioreactors and experimental devices for mechanobiological studies. Note that the applications of silicones are not limited to biomedical engineering. They are one of the key materials in recently emerging soft robotics [3]. Thanks to many promising rheological and mechanical properties such as low viscosity, high reproducibility, large deformability, low sensitivity to temperature, silicone-inspired filled polymers are major candidates in flexible stretch-sensors for healthcare applications, actuators in soft robotics and flexible materials for energy harvesting from ambient motions such as human walking and ocean and tidal waves [ref]. Moreover, due to low dissipative behaviour and low leakages characteristics, silicones and their composites have wide range of applications in aerospace industries [4].

Very recently, a commercially available silicone rubber, Ecoflex (Smooth-On, USA), becomes a typical elastomer for a wide range of practical applications. The two component room temperature curable silicone comes up with several Shore hardnesses ranging from Shore 00-10 to Shore 00-65. Strain sensors as epidermal electronic systems have widely been used nowadays where the mechanical compliance like human skin and a high stretchability are required. Due to low viscosities, high medical-grade, high reproducibility, silicone elastomers and their composites are idea candidates in the area of flexible stretch-based sensors. Amjadi et al. [5] made a super-stretchable, skin-mountable, and ultra-soft strain sensors by using Ecoflex-carbon nanotube nanocomposite thin films. They demonstrated that Ecoflex-based soft materials, where the sensing is enhanced by carbon nanotubes, have excellent hysteresis performance at different strain levels and rates with a high linearity and a small drift. Deep tissue injury caused by a prolonged mechanical loading disrupts blood flow and metabolic clearance. In order to mimic stress and strain in deep muscle tissues, the ability of Ecoflex is rigorously studied by Sparks et al. [6]. In this case, they conducted unconfined compression experiments on two different Shores, i.e., Ecoflex Shore 00-10 and Shore 00-30. The design of the actuation system is based on three fluidic chambers equally spaced in radial arrangement embedded in an Ecoflex matrix (Shore 00-50).

Despite increasing applications of Ecoflex in recent years, to the best of the authors' knowledge, a comprehensive thermo-viscoelastic investigation consisting of some critical experimentations, that are essential to quantify a typical viscoelastic material, are absent in the literature. Hence, in this study, we perform loading-unloading-reloading cyclic tests at different strain rates and strain levels, single-step relaxation tests with various strains and holding time, stress softening tests for identifying Mullins effect etc. These tests are conducted at various temperature profiles ranging from -40°C to 140°C. Since the material shows a significant stress recovery with time, a detailed study on the time-dependent stress recovery is presented. In contrast to other classical silicone polymers, Ecoflex shows some temperature-sensitive responses. The material shows a significant dissipative behaviour when tests are performed on virgin specimens. However, these dissipations are quickly disappeared in the case of repeated cycles. The same phenomenon is observed in single-step relaxation tests where virgin samples demonstrate pronounced viscous or recoverable non-equilibrium stresses. However, they are diminished once tests are conducted on pre-treated samples. Moreover, the material shows no residual strain upon reloading as well as it can recover stress softening almost fully after a sufficient long period of time.

The paper is organised as follows: in Sec. 2 a brief description is presented to outline the experimental

Figure 1. A 3D printed mould for sample preparation

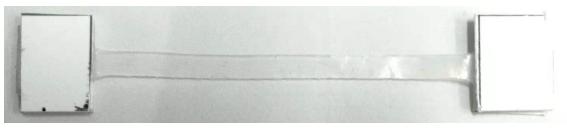

Figure 2. A typical specimen of 50 mm x 5 mm x 1 mm size that is attached with two grippers

set-up, procedures for sample preparations which are utilised to perform the experiments in our laboratory. In the following section Sec. 3, comprehensive experimental results are illustrated in detail, and sufficient analyses are given. In these cases, cyclic and relaxation behaviour of Ecoflex are extensively analysed. Furthermore, strain rate and temperature dependencies of the polymer are investigated and explained in the same section. Finally, section Sec. 4 summarises all major findings obtained in the study.

2. Experimental details

2.1. Specimen preparation

In this paper, Ecoflex$^{\text{TM}}$ silicone rubber of hardness Shore 00-30 is adopted for experimental investigations. Ecoflex is a platinum-catalyzed silicone mixed by two parts of liquid ingredients. In order to produce specimens in a desired shape, a mould is produced using a photosensitive resin with the help of a 3D printer. The mould is shown in Fig. 1. For uniaxial type tensile tests, rectangular specimens with 50 mm $\times$ 5 mm $\times$ 1 mm (length $\times$ width $\times$ thickness) are adopted mainly. Similar dimensions were chosen in previous experimental studies of various soft polymers in the case of uniaxial tensile tests, see [7, 8, 9, 10, 11]. However, for tests inside temperature chamber, due to the displacement constraint, 40 mm length specimens are adopted where specimens can be stretched maximally up to strain 400%.

To prepare Ecoflex samples, two liquid parts are mixed with 1:1 ratio and stirred well. The liquid mixture is then injected to the mould cavities by a syringe to control the volume of specimens. Afterwards, an extra degassing is carried out in a vacuumiser to guarantee the removal of trapped air bubbles. As per specifications of the Ecoflex supplier (Smooth-On), the curing time of the two component liquids should be four hours. However, we wait twelve hours so that specimens are fully cured into solid forms. Then they are demoulded smoothly. Note that Rey et al. [12] found in their investigations that specimens cured in room temperature were not fully crosslinked. Hence, they heated specimens at an elevated temperature for certain time to obtain a better crosslinking. They observed that such a temperature-enhanced curing of some silicones resulted in increased mechanical properties. Therefore, in our study, some specimens are further cured at 80°C for another four hours. Afterwards, we conduct a comparative study with samples cured under two different conditions. Results are presented in Sec. 3.1.

Note that due to extreme softness and stretchability of the Ecoflex polymer, the specimens show tendency to slide out from the grippers. Therefore, before mounting to the test machine, both ends of every specimen are adhered to plastic slices using silicone glue in case a specimen slides out of the grippers, as is shown in Fig. 2.

Figure 3. A complete thermo-viscoelastic testing system: ① is the main framework of the Instron 5567, ② is the control computer, ③ is the temperature chamber, ④ is the force sensor to monitor the applied force, and ⑤ is the crosshead of ①.

2.2. *Experimental set-up*

Extensive and systematic experimental characterizations are carried out on the Ecoflex silicone by an Instron 5567 universal test machine. For thermo-mechanical experimentations, the test machine is placed in a customized temperature chamber as shown in Fig. 3. A force sensor (④ in Fig. 3) of $\pm$50 N maximum capacity with a precision of 0.001 N is used. Temperature can be regulated inside a chamber (③ in Fig. 3) from -50°C to 150°C. The maximum loading speed of the machine crosshead (⑤ in Fig. 3) is 8 mm/s. The displacement limit of the machine without using the temperature chamber is 800 mm, while the limit is confined to 200 mm within the chamber. A Bluehill® universal user interface software on the control computer (② in Fig. 3) is utilized to interact with the machine and to extract experimental data.

In this paper, all stress results are presented as the first Piola (nominal) stress (i.e., the applied force divided by the initial undeformed cross-sectional area) against the corresponding nominal strain (i.e., applied displacement divided by the initial length of the specimen). Strain rates, mentioned in this contribution, are the time derivative of the nominal strain. In order to ensure the reproducibility of obtained results, more than three samples of each test condition are carried out and an averaging technique is applied to find the best data set. At least two hundred data points of each test are acquired from the software. For tests conducted inside the temperature chamber, oscillations in the data are observed due to the air circulation as the Ecoflex polymer is extremely soft material. Therefore, smoothing techniques are applied to reduce such noises. Before testing, the specimen is mounted between the upper and lower grippers and regulated at the target temperature for thirty minutes if necessary. In the following sections, the experimental procedures and related results covering major characterization techniques on Ecoflex of hardness Shore 00-30 will be discussed in detail.

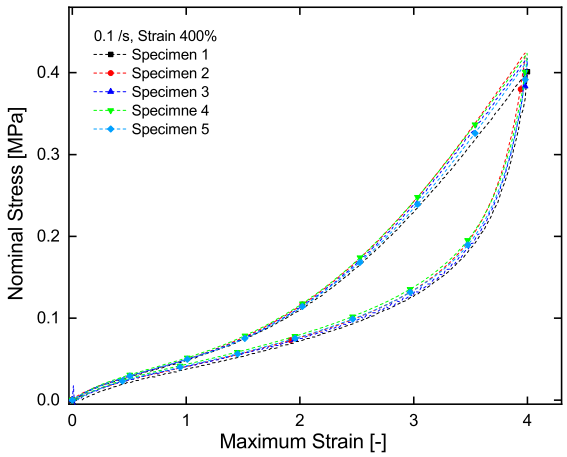

Figure 4. Reproducibility of test samples : Several cyclic tests are conducted at strain 400% under the sample loading protocols

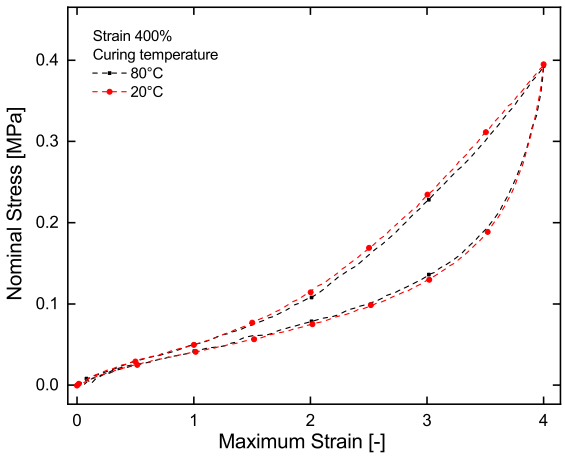

Figure 5. Temperature dependency on Ecoflex curing : Cyclic tests at strain 400% ; one cured at 20°C and another cured at 80°C

3. Experimental results

In this section, standard uniaxial tensile experimentations for thermo-viscoelastic characterization is performed on Ecoflex Shore 00-30. In addition, a variety of protocols of reloading tests are also conducted to investigate softening and recovery features of the material. Furthermore, some typical characteristics of soft polymers such as strain rate and temperature dependence are also covered in our study.

This section is arranged as follows. At first, a few tests to verify the reproducibility and the independence of cure conditions are carried out in Sec. 3.1. In Sec. 3.2, a couple of cyclic tests is firstly performed to characterise the hysteresis and strain-induced stress softening behaviour. Afterwards, in Sec. 3.3, a set of single-step relaxation tests are conducted to show the time-dependent behaviour of the material. Then the relationship between the stress softening and the stress relaxation is discussed, and the concepts of equilibrium stress and non-equilibrium stress are put forward. Based on these concepts, in Sec. 3.4, tests at different strain rates are carried out to inspect the rate dependence on both portions of stresses and to discuss the possible existence of viscoelasticity. In addition, in Sec. 3.5, the influence of temperature on both portions are also discussed. Finally in Sec. 3.6, the stress recovery is rigorously investigated on stretched specimens after different recovery times. Apart from the temperature tests in Sec. 3.5, all tests in this section are carried out at ambient temperature (20° C). Furthermore, except the strain rate tests presented in Sec. 3.4, all tests are performed at a strain rate of 0.1 /s.

3.1. Reproducibility tests

Prior to actual experiments, the reproducibility of material samples is verified by applying the same test protocol to at least five different specimens. From Fig. 4, it can be observed that only small fluctuations exist among manually produced specimens within an acceptable scale. As is mentioned above, to evaluate the influence of crosslinking effects at different temperatures, some specimens are additionally cured at 80°C for four hours. Fig. 5 illustrates that the curing temperature does not have any considerable influence on the mechanical stress response.

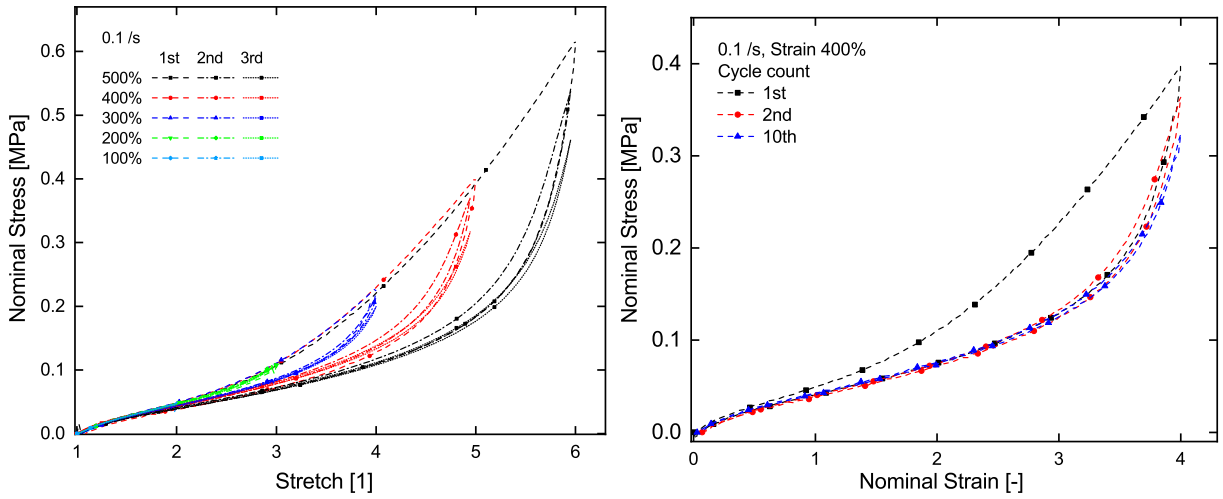

(a)

(b)

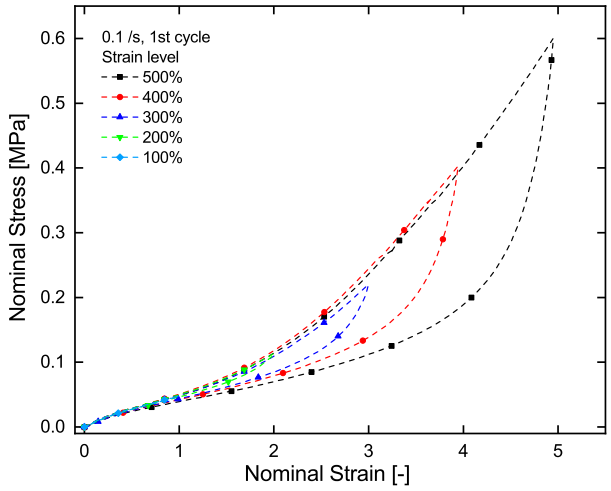

(c)

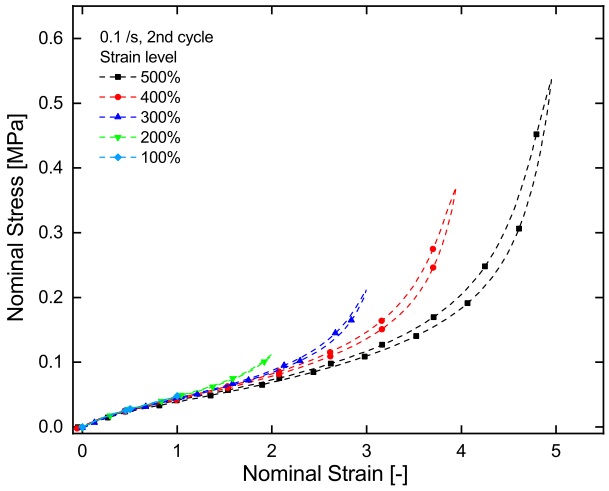

(d)

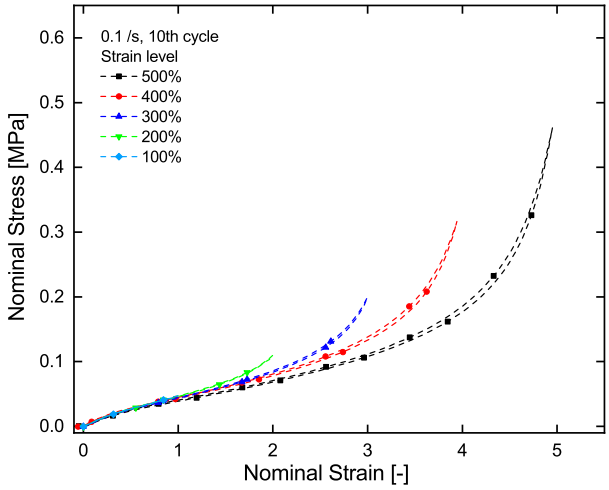

(e)

Figure 6. Cyclic tests at five different strain levels. (a) Stress results with third cycles, (b) test results of a sample at strain 400% after ten repeated cycles, (c) only first cycles of tests at different strain levels, (d) the second cycles, (e) the tenth cycles.

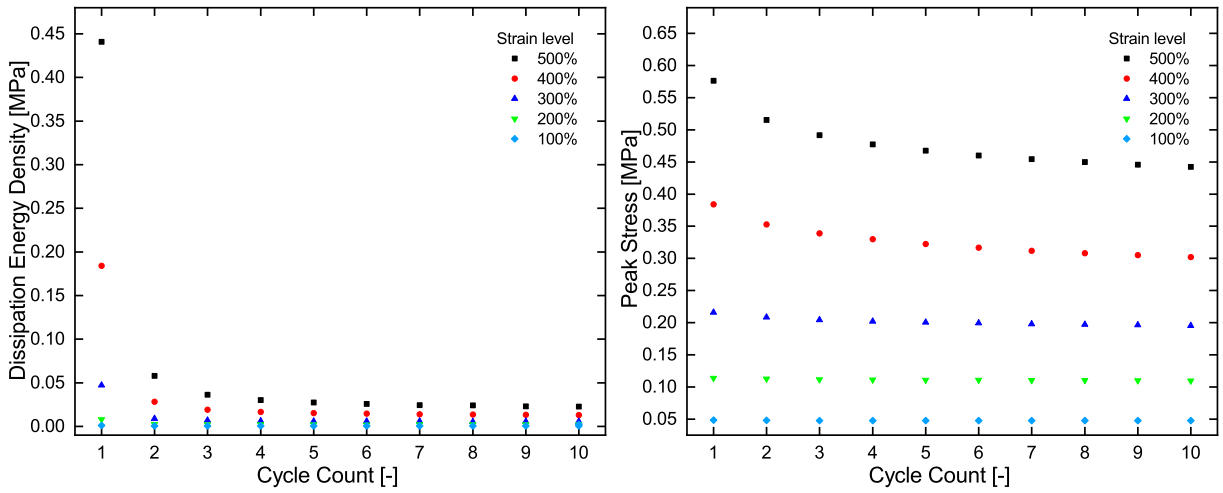

Figure 7. Peak stress and dissipation energy density produced by cyclic tests at different strain levels with multiple cycles. (a) dissipation energy density versus cycle count, (b) peak stress versus cycle count.

3.2. Cyclic behaviour

In order to characterize the basic loading and unloading behaviour of Ecoflex (Shore 00-30), cyclic tests are performed on five different specimens at strain levels of 100%, 200%, 300%, 400%, and 500%, respectively, with ten repeated cycles each. For all tests, a strain rate of 0.1 /s is selected where the results are illustrated in Fig. 6.

Fig. 6(b) shows test results of a sample at strain 400% with ten repeated loading-unloading cycles. On the primary loading path (the black dash curve with square symbol), the material follows a typical nonlinear stress-stretch behaviour on a virgin specimen (without any mechanical pre-treatments). The stiffness decreases slightly and stabilises quickly at the beginning of the loading path. Afterwards, it transforms into an upturned pattern from strain 80%. Compared to the primary loading path, each reloading path in the second (the red dash curve with circle symbol) and the following cycles (e.g., the blue dash curve with triangle symbol) experiences an apparent stress reduction, and exhibits a stronger nonlinearity with a 'S' shape. The stiffness plateau extends significantly, and at a strain close to the maximum of the previous strain, stress increases rapidly and almost joins back to the primary curve, which is described as the 'strain hardening' [13]. This stress reduction behavior is called the stress softening or the Mullins effect [14]. At the subsequent cycles after the first one, the softening still occurs, but it is insignificant compared to the first one and the responses between cycles and between loading and unloading paths tend to coincide. Note that before strain 100%, the stress softening is negligible. Fig. 6(c), Fig. 6(d) and Fig. 6(e) compare the first, the second, and the tenth cycles at different strains. From each figure, it can be seen that with a higher maximum strain level, the stress level in the unloading or the reloading path decreases progressively at a particular strain, indicating that the stress softening behaviour is a strain-induced phenomenon.

Fig. 7 illustrates the peak stress and hysteresis responses of the tests presented in Fig. 6. The stress softening behaviour causes a gap between the loading and unloading paths. This gap forms a hysteresis loop and contributes to the dissipation energy density, which is calculated as the closed area inside the loading and

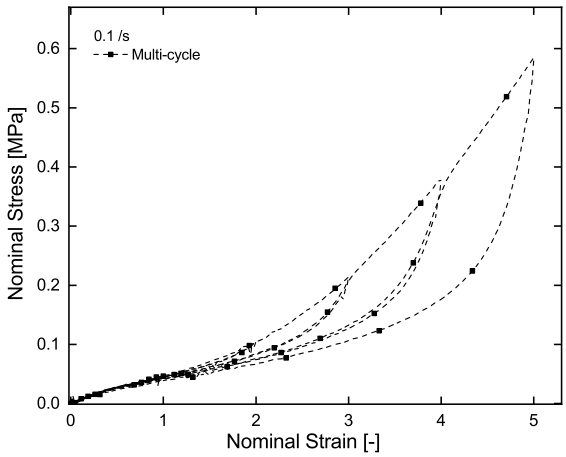

Figure 8. A multiple cyclic test with increasing strain lev- els.

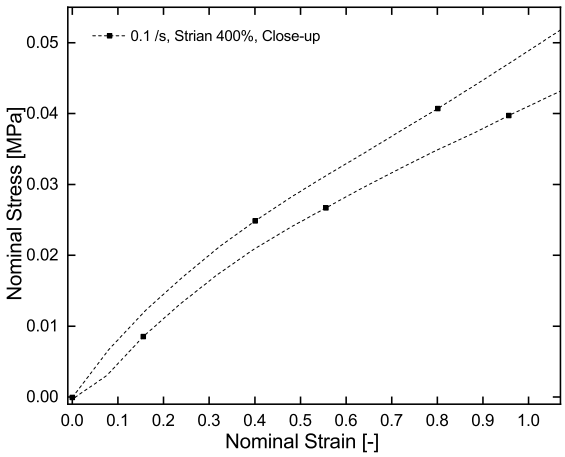

Figure 9. A zoom-in graph for a cyclic test at strain 400%.

unloading path l, i.e., $\int_l \sigma \mathrm{d}\varepsilon$, where σ and ε are the nominal stress and nominal strain, respectively. The level of stress softening can be evaluated by the dissipation energy density. Fig. 7(a) clearly shows that the hysteresis decreases progressively with more cycles. The decrease mainly happens between the first and the second cycles, and stabilises at a very low level soon in the subsequent cycles. Note that the hysteresis caused by the stress softening, i.e., the part that is removed in the subsequent cycles, and that caused by viscoelasticity, i.e, the part remains, should be distinguished. A tiny amount of hysteresis after ten cycles' at each strain level may indicate a minimal level of viscoelasticity. However, this is neither the main feature of Ecoflex polymer nor the primary response of the material. Fig. 7(b) plots the change of the peak stress (the stress at the maximum strain) with a cycle count. When a specimen is reloaded with more cycles, the peak stress experiences a reduction and tends to stabilise as well. At a smaller maximum strain, the reduction is smaller and stabilises at an earlier cycle. This pattern shares a resemblance of the relaxation behaviour. In fact, stress relaxations undergo during the loading and unloading processes. Hence, the peak stress decreases with repeated cycles. This behaviour is called the cyclic relaxation [15, 16, 17, 18]. In contrast, the normal stress relaxation, where a specimen is held fixed after a certain strain, is called the static relaxation.

A test of multiple cycles with a 100% increment of strain is performed as is shown in Fig. 8. Therein, a curve of the single cycle test serves as an envelope of the curve of this multi-cycle test. Each of the reloading paths reaches the maximum stress of the former cycle. This characteristic is also an evidence of the strain-induced softening and is a typical outcome of the Mullins effect [19, 14, 20, 21, 22, 23, 24, 25, 26].

Furthermore, it is observed that upon unloading, specimens come back to their original configurations, regardless of the strain level and the cycle count, as is shown in Fig. 9 in a close-up look. In the next section, further discussions will be carried out where it will be concluded that the residual strain even after the unloading of a relaxation test is also negligible. This behaviour of hysteresis indicates the differences of Ecoflex from a typical viscoelastic material.

3.3. Relaxation behaviour

Stress relaxation is one of the key phenomena to identify the time-dependent behaviour of any polymeric material. Firstly, a relaxation test is performed where a sample is elongated at strain 400% with the max-

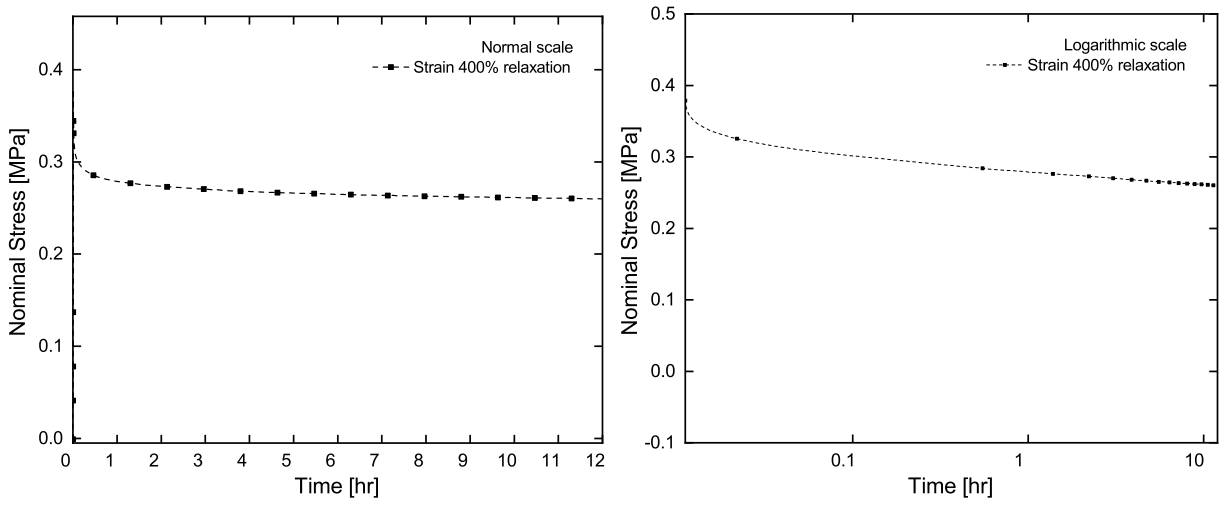

(a) (b)

Figure 10. A twelve-hour relaxation tests at strain 400%. (a) On a linear time axis, (b) on a logarithmic time axis.

imum crosshead speed of the machine (8 mm/s) and let it relax. The test results are plotted on a linear time scale in Fig. 10(a) as well as in a logarithmic time scale in Fig. 10(b). The virigin material exhibits a significant stress relaxation behaviour. Note that even though it seems an equilibrium stress (the stress after the entire removal of the time-dependent portion) is reached under a linear time scale, a logarithmic time scale gives us a better picture that a declining trend still exists even after twelve hours of relaxation. Hence, a sample might take a longer time to reach the actual equilibrium stress. In the following section, all relaxation tests are plotted on a logarithmic time scale. Since there is only a small stress reduction between three hours and twelve hours relaxations, for experimental simplicity, all relaxation experiments that follow hereafter will be carried out with a three-hour holding time.

Now more single-step relaxation tests on virgin Ecoflex specimens at strains from 100% to 500% with strain 100% interval are conducted. Fig. 11(a) illustrates the stress relaxations over the holding time on a logarithmic time scale, while Fig. 11(b) illustrates the same in a stress-strain format. As the time evolves, the stress attenuates and tends to reach a stable value; the equilibrium stress. A larger strain results in a greater stress reduction from the peak stress to the equilibrium stress and a longer relaxation time to reach the equilibrium stress. At larger strains such as 400% and 500%, declining tendencies of the stresses still exist over three hours' of relaxations. It means that the actual equilibrium stresses are smaller than the current relaxation stresses (the stress at actual stage of relaxation time).

Given that the stress softening is significantly a strain-induced phenomenon for Ecoflex, as is mentioned in Sec. 3.2, few relaxation tests are carried out after several cycles of pre-stretch at various strains. In Fig. 12, all specimens are pre-stretched at a strain 500% for one cycle, and then they are allowed to relax at different strains starting from 100% up to 500%. Due to the 500% pre-stretch, stress softening occurs prior to actual stress relaxations. For the tests from strains 100% to 400%, it can be observed that all the stresses only experience a minimal decrease where most of the stress drops happen within a few minutes. Even though we plot stress evolutions on the logarithmic time axis as in Fig. 12(a), there is only a slight declining tendency. After the pre-stretch at a larger strain and the consequent stress softening, most of the non-equilibrium stresses

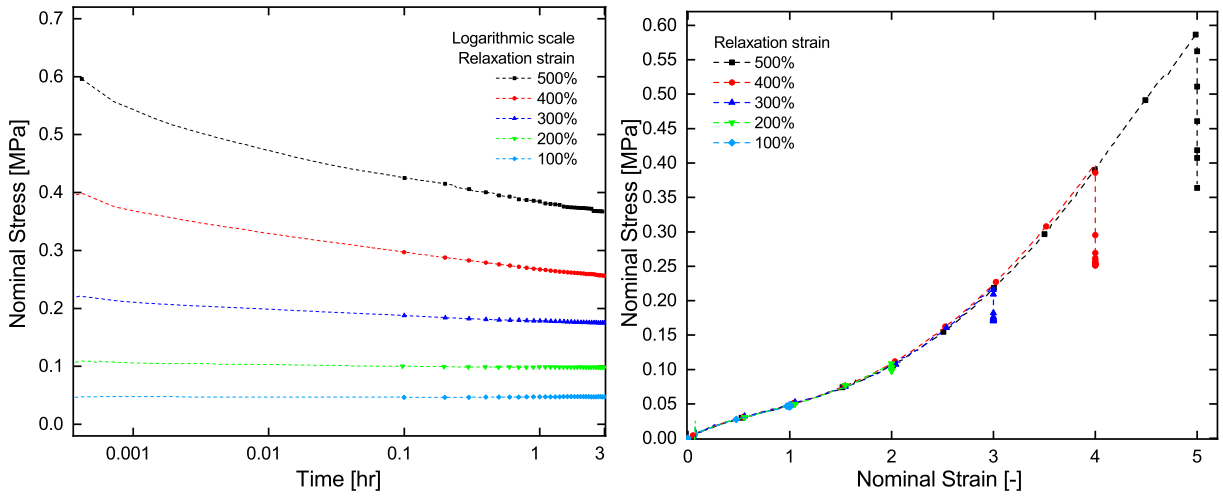

(a) (b)

Figure 11. Three-hour relaxation tests at different relaxation strains. (a) Stress evolution curves plotted on a logarithmic time axis, (b) stress-strain curves.

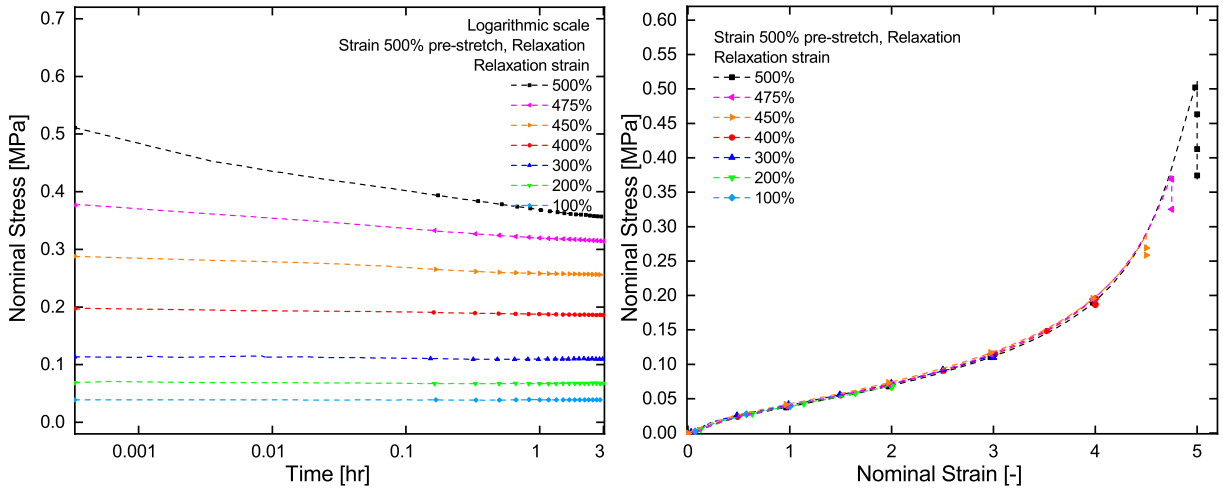

(a) (b)

Figure 12. Three-hour relaxation tests with a pre-stretch of strain 500% at different relaxation strains. (a) Stress evolution plotted on a logarithmic time axis, (b) stress-strain curves.

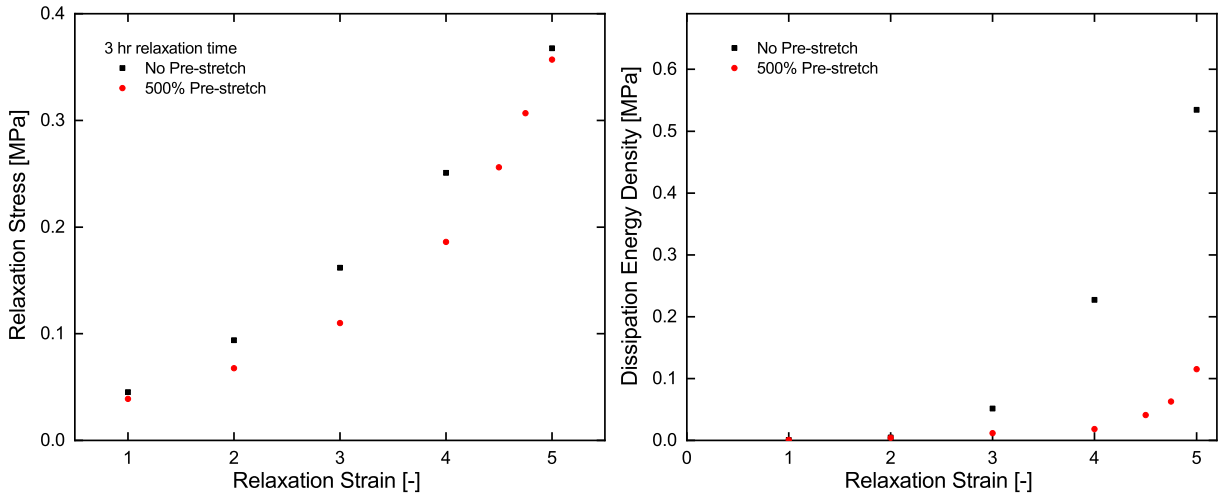

Figure 13. Comparison between three-hour relaxation tests with and without a pre-stretch of strain 500%. (a) Relaxation stress at different relaxation strains, (b) dissipation energy density at different relaxation strains after unloading.

are almost removed. Additional tests over 400%, i.e. 450%, 475%, 500%, are also performed. For these cases, when the relaxation strain approaching the value of the pre-stretch, the stress relaxation gets more pronounced.

Fig. 13(a) compares the relaxation stresses of the tests with and without the pre-stretch at a strain 500%. With an increase of the applied relaxation strain, the difference of relaxation stresses between the tests with and without a pre-stretch enlarges and then shrinks near the strain level of pre-stretch. This pattern is similar to the difference in the cyclic responses between a virgin and a pre-stretched specimens. A larger strain softening contributes to a lower relaxation stress. Fig. 13(b) compares the dissipation energy densities of the two tests. Here, the energy density is calculated by the closed area surrounded by the loading, relaxation and unloading path in the stress-strain curve of a relaxation test, such as Fig. 14(a). It can be seen that the hysteresis is removed significantly with a pre-stretch, similar to the results in multi-cyclic tests.

It is noteworthy that even an unloading after the relaxation of several hours, strains can recover completely right after the applied force is released, see Fig. 14(b). This fact gives us a clue that the stress softening and the relaxation are possibly not resulted from any viscoelasticity. Typically, a recoverable residual strain exists right after an unloading since strain and stress responses are not fully synchronized for a typical viscoelastic material.

Since it is observed that the relaxation does not proceed fully at a plateau even after twelve hours of relaxation, the equilibrium stress is not fully identified. Bearing in mind that a pre-stretch can largely remove the relaxation behaviour, one may consider that the equilibrium stress may be achieved earlier by applying a larger pre-stretch without waiting for a long- time relaxation. On these grounds, relaxation tests with a cycle of pre-stretch at various strain levels larger than applied relaxation strains are carried out, see Fig. 15. By plotting the stress evolutions again on a logarithmic time axis, it is revealed that with a larger pre-stretch, a relaxation test begins with a low peak stress, and then the stress relaxes quickly to a lower level. How-

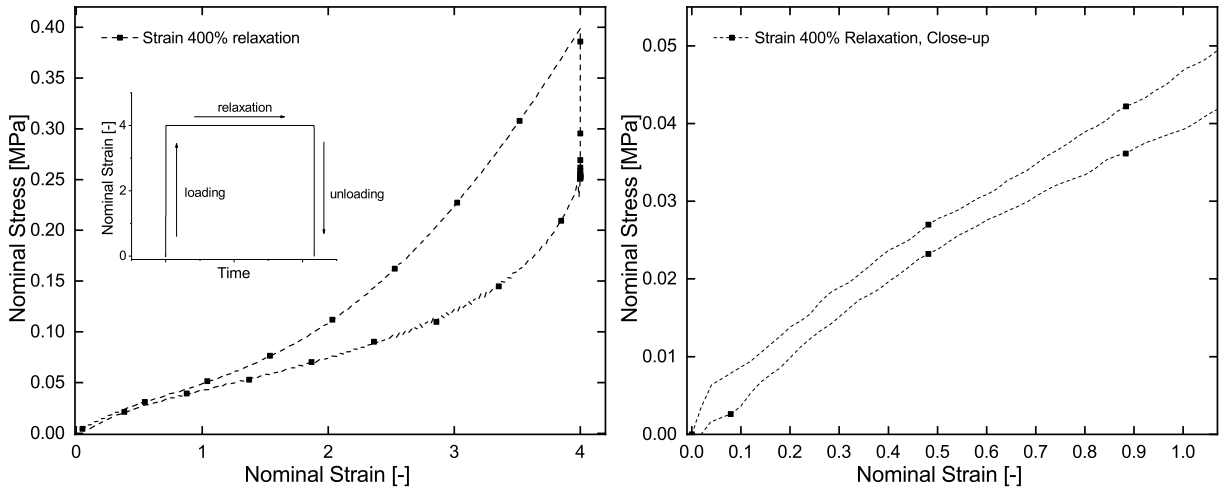

(a) (b)

Figure 14. A relaxation test with the unloading path. (a) The whole view, (b) a close-up look.

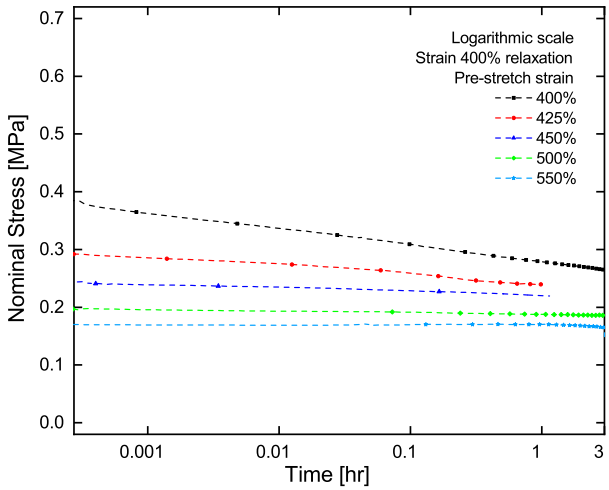

Figure 15. Three-hour relaxation tests at strain 400% with different levels of pre-stretch.

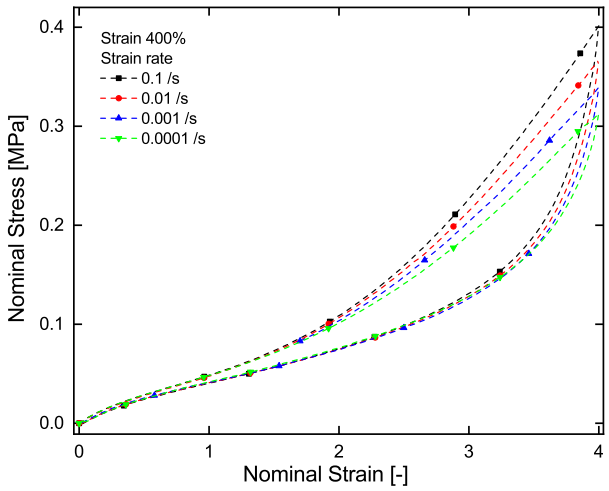

Figure 16. Cyclic tests at different strain rates with a strain 400%

ever, from the tendency of these curves, a smaller pre-stretch retains a larger slope of the stress reduction, indicating that there is a possibility that after an infinite time period, all the stresses converge at the same value, i.e., the equilibrium stress, regardless of the strain level of the pre-stretch. Under such an assumption, the equilibrium stress is irrelevant to the pre-stretch level, and the softening caused by the pre-stretch takes the place of a portion of relaxation. A pre-stretch can simply be an easier way in obtaining the equilibrium stresses.

3.4. Strain rate dependence

In the previous sections, the relaxation, a time-dependent phenomenon, is observed. Therefore, it can be envisaged that a strain rate-dependent phenomenon can also exist. In order to quantify the strain rate dependence of the polymer, load-unloading-reloading cyclic tests at different strain rates are carried out. It is interesting to note that virgin specimens clearly demonstrate strain rate dependence beyond strain 200%. For example, at strain 400% from 0.0001 /s to 0.1 /s strain rates with a four decades difference, the ultimate stress increases from 0.3 MPa to 0.4 MPa, see Fig. 16.

Fig. 17(a) shows that a higher strain rate brings a higher stress value at the first few cycles. However, with the increase of number of cycles, the peak stress decreases quickly and tends to reach the same value as the ones of lower rates. This is again partially due to the cyclic relaxation response. Similar to the static relaxation, a higher strain rate only leads to a higher peak stress but a faster stress reduction and the same equilibrium stress. Fig. 17(b) shows that a higher strain rate leads to a larger hysteresis at the first cycle thanks to the time dependent behaviour. Here, due to the softening behaviour, from the second cycles the dissipation energies are almost the same at different strain rates.

When the time-dependent non-equilibrium portion is removed by pre-treatments, the time or rate dependence behaviour will disappear right afterwards, as is mentioned in Sec. 3.3. In Fig. 18, we compare two reloading curves at strain 400% with two different strain rates after three different types of pre-treatments: a larger pre-stretch of 500% (Fig. 18(a)), a relaxation test at 400% (Fig. 18(b)), a strain with multiple cycles at 400% (Fig. 18(c)). Even though the strain rates in the graphs are 500 times, 400 times, and 100 times different, respectively, all two curves in each graph are almost overlapped. This result supports our assump-

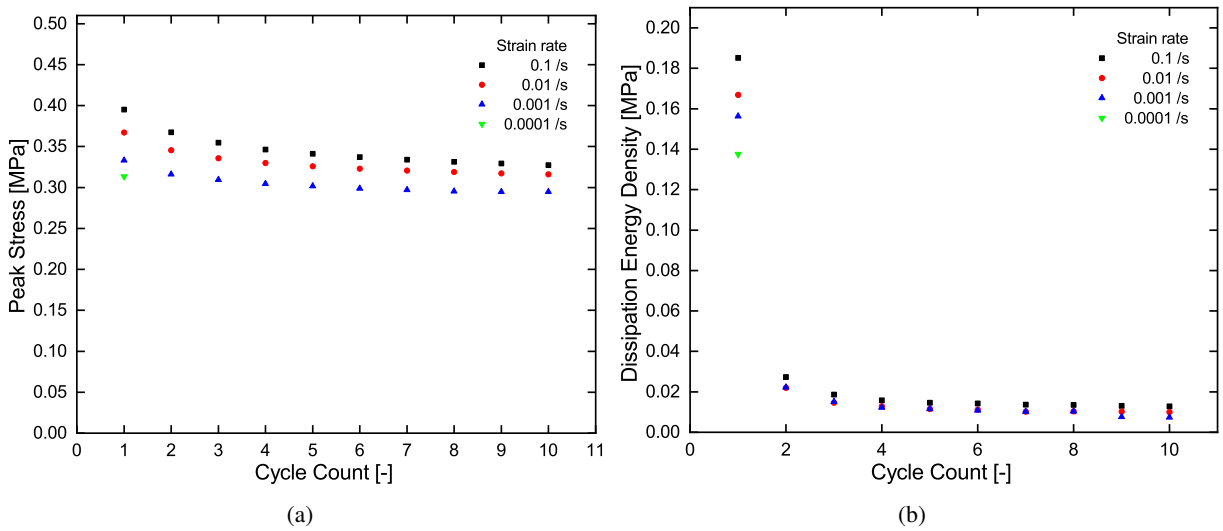

(a) (b)

Figure 17. Peak stress and dissipation energy density of cyclic tests at different strain rates with multiple cycles. (a) Peak stress versus cycle count, (b) dissipation energy density versus cycle count.

tion that the stress softening by loading-unloading cyclic tests, static and cyclic relaxations have the similar stress reduction effects. This fact also shows that after removal of the non-equilibrium stress by any of the three processes, the stress obtained does not depend on time. Hence, we can term the stress as the equilibrium one. Furthermore, for a viscoelastic material, in addition to the stress reduction thanks to the relaxation during the loading path, a common phenomenon is that the stress increases during the strain holding period on an unloading path [27, 20, 28]. This phenomenon is not observed for the case of Ecoflex silicone rubber. Therefore, it can be concluded that Ecoflex does not demonstrate significant viscoelasticity behaviour.

3.5. Temperature dependence

In the previous sections, we observe that the stress of the material consists of two parts: an equilibrium stress portion and a non-equilibrium stress part. In this section, similar to the investigation of the strain rate dependence, the influences of temperature on these two stress portions are also tested, respectively. Several researches illustrate that mechanical properties of silicone polymers are sensitive to temperature variations [12, 29, 30]; although such types of dependence are not as pronounced as other polymers such as acrylics [31]. Therefore, we have conducted a couple of cyclic tests within the temperature chamber. Tests performed at different temperatures with a strain of 400% are presented in Fig. 19, which shows that the polymer is somehow temperature-sensitive. Before strain 250%, the stress values increase as the temperature increases, while over strain 250% the opposite trend is observed, i.e., the stress level decreases as the temperature increases. Moreover, the hysteresis decreases as the temperature increases.

Note that tests at 140°C temperature undergo failures in the gauge section of the specimen with a good reproducibility. Due to the displacement limit of the machine while tests are being performed within the temperature chamber, it is a challenging task to perform failure tests with a larger ultimate extension at a lower temperature. Nevertheless, these results give us a glimpse of the fact that the material failure is also dependent on temperature, and it could be predicted that a higher temperature leads to a smaller ultimate extension before a failure.

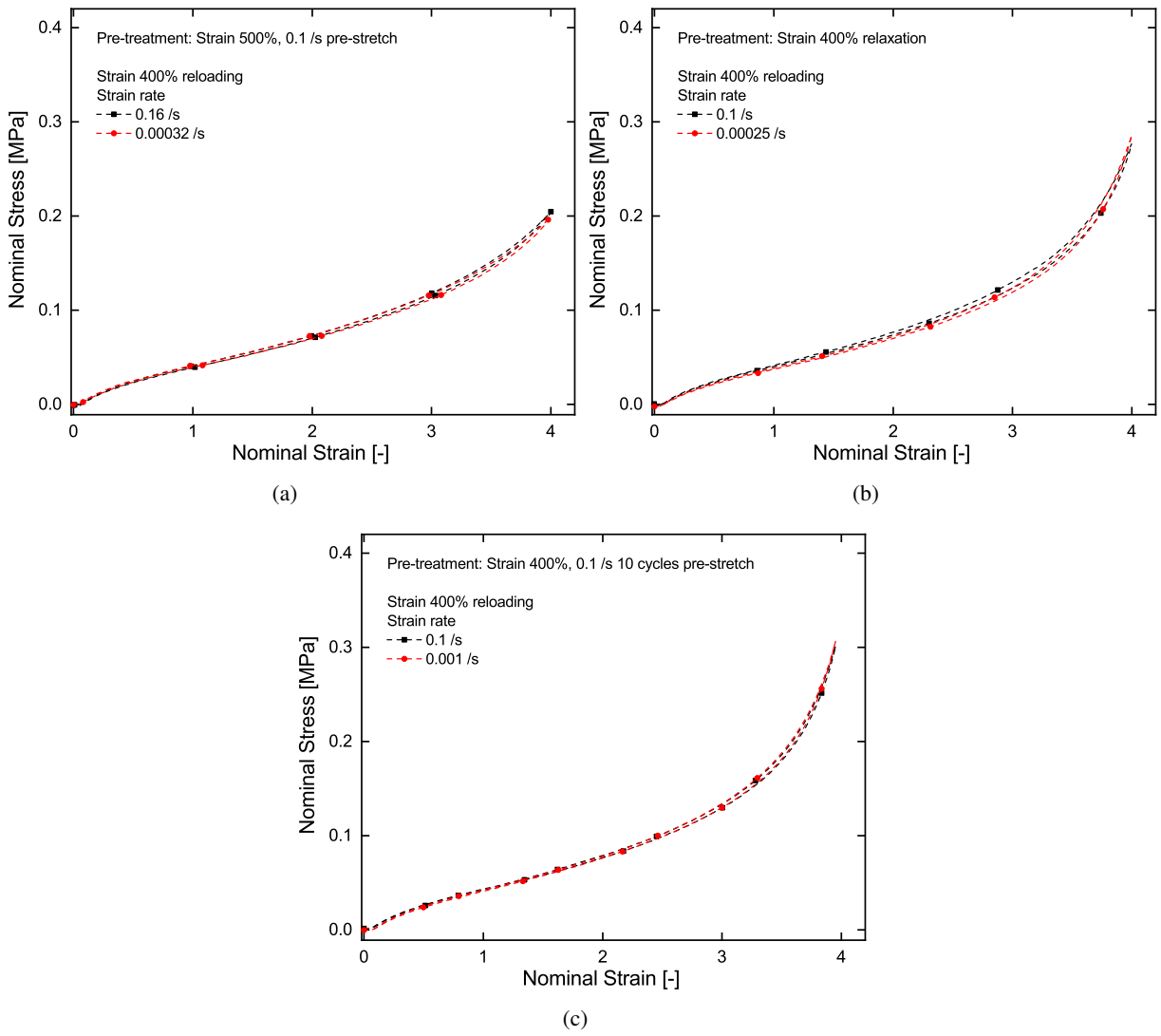

Figure 18. Cyclic tests at different strain rates after different types of pre-treatments. (a) Pre-stretch at strain 500%, (b) relaxation at strain 400%, (c) ten cycles pre-stretch at strain 400%.

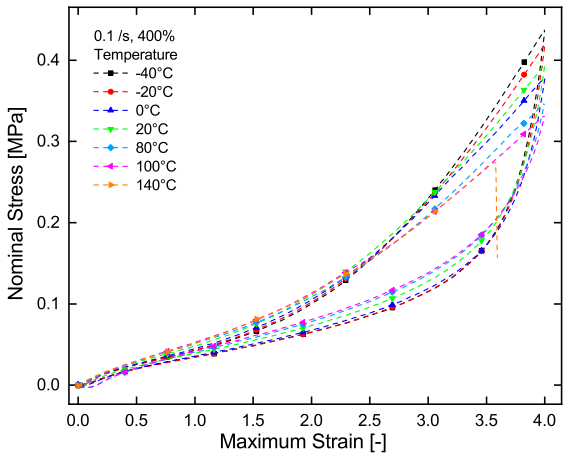

Figure 19. Cyclic tests at various temperatures at a strain 400%

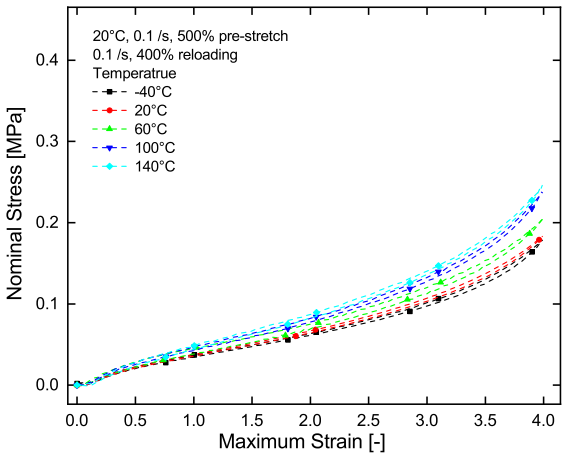

Figure 20. Cyclic tests at various temperatures for a strain 400% where the pre-stretch is conducted at room temperature with a strain of 500%

In order to see what exactly happens to the non-equilibrium stress portion, the equilibrium stress portion should closely be monitored too. Fig. 20 illustrates the tests at different temperatures and at a strain of 400% with a 500% pre-stretch. It can be seen that the hysteresis is almost removed. From a lower temperature to ambient and then to elevated temperature, the stress level undergoes a progressive increase. Note that in Sec. 3.2, it is found that the hysteresis is small before strain 200%, indicating that the equilibrium stress plays a dominant part at this strain range. This explains the increase of stress with the increasing temperature of total stress. After strain 250% or so, the time-dependent non-equilibrium stress overtakes the equilibrium stress. Therefore, the total stress exhibits a decreasing trend at a higher temperature. Finally, it can be concluded that with the temperature increasing, the equilibrium stress increases and the non-equilibrium stress decreases.

3.6. Stress recovery

Although many soft materials exhibit similar stress softening behaviour as Ecoflex silicone rubbers described in the previous sections, the extent of stress recovery varies from material to material [32, 22, 23, 33, 34, 35]. In this section, the recovery behaviour of Ecoflex is investigated in detail.

In Fig. 21, the stress recovery behaviour is depicted. All specimens are pre-stretched beforehand, and then each specimen is reloaded after different recovery times at a stress-free state. Fig. 21(a) shows that the stress level of the first reloading cycle increases along the loading path with a longer recovery period. This indicates that the stress softened in the non-equilibrium portion will recover as time passes. For the first reloading cycle, the hysteresis (black points in Fig. 21(b)) also show recovering trends. The hysteresis after the recovery for a month is still far from that of a virgin specimen although it continuously maintains an increasing trend. Some researches suggest that such softening is partly recoverable and partly unrecoverable [23, 35, 34]. However, there is also a possibility for Ecoflex that the hysteresis reduction and stress reduction can recover fully after a 'sufficient long time'.

Since we have presumed that the stress relaxation imposes similar influences on Ecoflex as the stress softening, one can predict that the relaxation could also recover with time. In a relaxation test of the material,

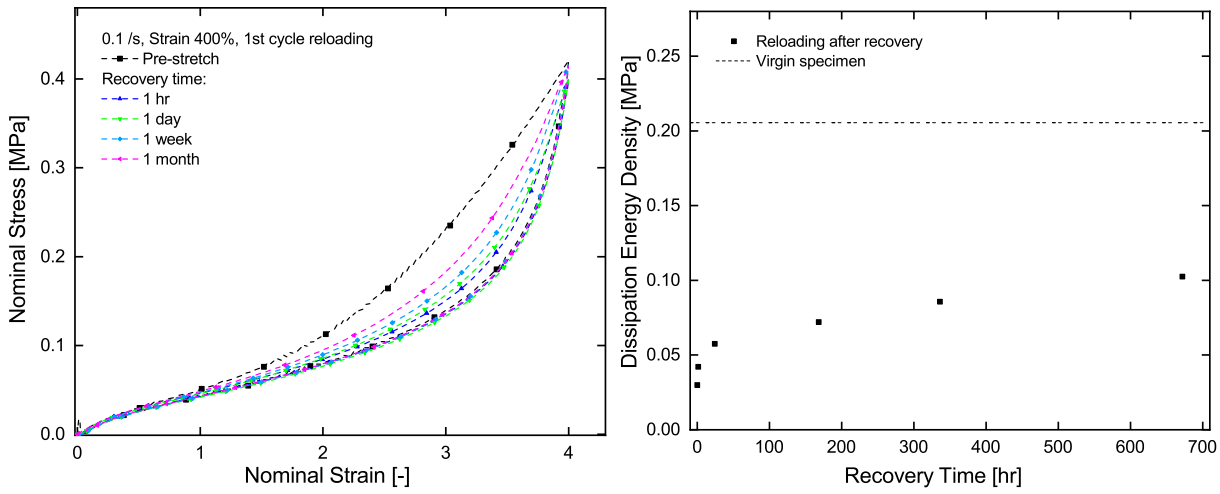

(a) (b)

Figure 21. Reloading of pre-stretched specimens after different recovery periods. (a) Stress-strain curves, (b) dissipation energy density.

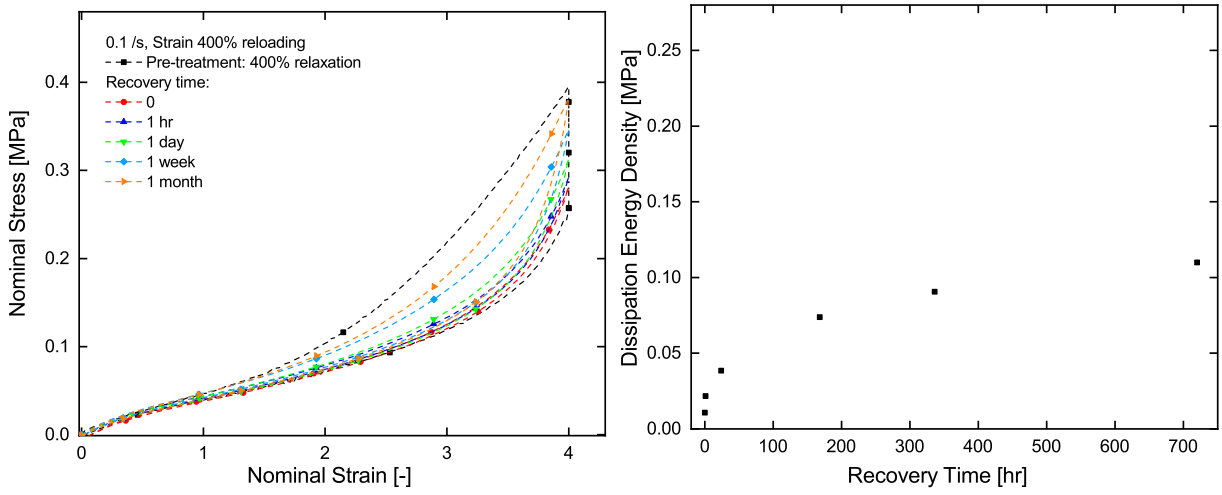

(a) (b)

Figure 22. Reloading of relaxed specimens after different recovery periods. (a) Stress-strain curves of relaxation and reloading, (b) dissipation energy density of reloading.

stress decreases significantly. The immediate reloading curve is also close to the unloading path right after relaxation in Fig. 22(a). After recovery for a week, the hysteresis of the reloading cycle show obvious recovery. It is also illustrated in Fig. 22(b). It can also be observed that with time increases, the stress level at loading and unloading path and the peak stress will recover to a certain degree, which is similar to the recovery after the stress softening. Overall, a major stress recovery is witnessed in the non-equilibrium portion of the stress after any types of softening.

4. Conclusions

In this study, we focus on the characterization of the thermo-mechanical behaviour of a widely used silicone rubber, i.e., Ecoflex of Shore 00-30. A comprehensive and systematical mechanical experimentation is carried out including cyclic loading-unloading tests with multiple cycles, relaxation tests, reloading tests after recovery, strain rate and temperature dependence tests. After a rigorous study on Ecoflex, following summary can be drawn:

- A significant strain-induced stress softening phenomenon is observed. A time-dependent relaxation behaviour is also observed. It is found that any pre-treatments either by applying multiple cycles or a pre-stretching at a higher strain, or relaxing the specimen at a specific strain can cause a significant stress decrease and the removal of hysteresis. The corresponding stress softening and relaxation share a similarity on the material response, and they may be attributed to some micro-mechanical causes such as polymer chain breakages.
- Based on the experimental results, it is assumed that the total stress could be decomposed into two parts: an equilibrium stress portion that is time-independent, and a non-equilibrium stress portion which is time-dependent.
- The non-equilibrium stress portion can be removed by stress softening, static relaxation or cyclic relaxation. This portion is significantly recoverable with time. A possibility is that all the stress softened or relaxed in this non-equilibrium portion could recover completely after a long enough time under a stress-free state.
- No residual strain is observed, and no pronounced strain rate dependence is found after the removal of the non-equilibrium stress portion. This implies that the material may not be a typical viscoelastic polymer.
- Temperature dependence is observed to some extends. The equilibrium stress increases as temperature increases, while the non-equilibrium stress and the consequent hysteresis decrease as the temperature increases.

In a forthcoming contribution, we will characterize Ecoflex of other Shore hardnesses using similar protocols illustrated in this study. Furthermore, we are working to develop constitutive models that can capture the time-dependent stress softening and recovery behaviour of Ecoflex.

Acknowledgements

The first two authors would like to extend their sincere appreciation to Zienkiewicz Centre for Computational Engineering (ZCCE), Swansea University, UK for supporting the work. This support facilitates an exchange visit of the first author to ZCCE.

References

[1] J. S. Bergstroem, Large strain time-dependent behavior of elastomeric materials, Phd dissertation, Massachusetts Institute of Technology, USA (1999).

[2] H. Hoeksema, M. D. Vos, J. Verbelen, A. Pirayesh, S. Monstrey, Scar management by means of occlusion and hydration: A comparative study of silicones versus a hydrating gel-cream, Burns 39 (7) (2013) 1437–1448. doi:10.1016/j.burns.2013.03.025.

[3] S. Zakaria, L. Yu, G. Kofod, A. L. Skov, The influence of static pre-stretching on the mechanical ageing of filled silicone rubbers for dielectric elastomer applications, Materials Today Communications 4 (2015) 204–213. doi:10.1016/j.mtcomm.2015.08.002.

[4] L. Guo, Y. Lv, Z. Deng, Y. Wang, X. Zan, Tension testing of silicone rubber at high strain rates, Polymer Testing 50 (2016) 270–275. doi:10.1016/j.polymertesting.2016.01.021.

[5] M. Amjadi, Y. J. Yoon, I. Park, Ultra-stretchable and skin-mountable strain sensors using carbon nanotubes–ecoflex nanocomposites, Nanotechnology 26 (37) (2015) 375501. doi:10.1088/0957-4484/26/37/375501.

[6] J. L. Sparks, N. A. Vavalle, K. E. Kasting, B. Long, M. L. Tanaka, P. A. Sanger, K. Schnell, T. A. Conner-Kerr, Use of silicone materials to simulate tissue biomechanics as related to deep tissue injury, Advances in Skin & Wound Care 28 (2) (2015) 59–68. doi:10.1097/01.asw.0000460127.47415.6e.

[7] M. Hossain, D. K. Vu, P. Steinmann, Experimental study and numerical modelling of VHB 4910 polymer, Computational Materials Science 59 (2012) 65–74. doi:10.1016/j.commatsci.2012.02.027.

[8] M. Johlitz, H. Steeb, S. Diebels, A. Chatzouridou, J. Batal, W. Possart, Experimental and theoretical investigation of nonlinear viscoelastic polyurethane systems, Journal of Materials Science 42 (23) (2007) 9894–9904. doi:10.1007/s10853-006-1479-4.

[9] Z. Liao, M. Hossain, X. Yao, M. Mehnert, P. Steinmann, On thermo-viscoelastic experimental characterization and numerical modelling of VHB polymer, International Journal of Non-Linear Mechanics 118 (2020) 103263. doi:10.1016/j.ijnonlinmec.2019.103263.

[10] M. Wissler, E. Mazza, Mechanical behavior of an acrylic elastomer used in dielectric elastomer actuators, Sensors and Actuators A: Physical 134 (2) (2007) 494–504. doi:10.1016/j.sna.2006.05.024.

[11] R. Sahu, K. Patra, J. Szpunar, Experimental study and numerical modelling of creep and stress relaxation of dielectric elastomers, Strain 51 (1) (2014) 43–54. doi:10.1111/str.12117.

[12] T. Rey, G. Chagnon, J.-B. L. Cam, D. Favier, Influence of the temperature on the mechanical behaviour of filled and unfilled silicone rubbers, Polymer Testing 32 (3) (2013) 492–501. doi:10.1016/j.polymertesting.2013.01.008.

[13] G. Chagnon, On the relevance of continuum damage mechanics as applied to the mullins effect in elastomers, Journal of the Mechanics and Physics of Solids 52 (7) (2004) 1627–1650. doi:10.1016/j.jmps.2003.12.006.

[14] L. Mullins, Softening of rubber by deformation, Rubber Chemistry and Technology 42 (1) (1969) 339–362. doi:10.5254/1.3539210.

[15] G. Weng, Cyclic stress relaxation of polycrystalline metals at elevated temperature, International Journal of Solids and Structures 19 (6) (1983) 541–550. doi:10.1016/0020-7683(83)90091-4.

[16] M. Gunawan, L. Davila, E. Wong, S. Mhaisalkar, T. Tsai, S. Osiyemi, Static and cyclic relaxation studies in nonconductive adhesives, Thin Solid Films 462-463 (2004) 419–426. doi:10.1016/j.tsf.2004.05.049.

[17] D.-Y. Chiang, Modeling and characterization of cyclic relaxation and ratcheting using the distributed-element model, Applied Mathematical Modelling 32 (4) (2008) 501–513. doi:10.1016/j.apm.2007.01.002.

[18] S.-L. Zhang, F.-Z. Xuan, Interaction of cyclic softening and stress relaxation of 9–12% cr steel under strain-controlled fatigue-creep condition: Experimental and modeling, International Journal of Plasticity 98 (2017) 45–64. doi:10.1016/j.ijplas.2017.06.007.

[19] L. Mullins, N. R. Tobin, Theoretical model for the elastic behavior of filler-reinforced vulcanized rubbers, Rubber Chemistry and Technology 30 (2) (1957) 555–571. doi:10.5254/1.3542705.

[20] J. S. Bergstroem, M. C. Boyce, Constitutive modeling of the large strain time-dependent behavior of elastomers, Journal of the Mechanics and Physics of Solids 46 (5) (1998) 931–954. doi:10.1016/S0022-5096(97)00075-6.

[21] I. Stevenson, L. David, C. Gauthier, L. Arambourg, J. Davenas, G. Vigier, Influence of SiO2 fillers on the irradiation ageing of silicone rubbers, Polymer 42 (22) (2001) 9287–9292. doi:10.1016/s0032-3861(01)00470-0.

[22] D. E. Hanson, M. Hawley, R. Houlton, K. Chitanvis, P. Rae, E. B. Orler, D. A. Wrobleski, Stress softening experiments in silica-filled polydimethylsiloxane provide insight into a mechanism for the mullins effect, Polymer 46 (24) (2005) 10989–10995. doi:10.1016/j.polymer.2005.09.039.

[23] J. Diani, B. Fayolle, P. Gilormini, A review on the mullins effect, European Polymer Journal 45 (3) (2009) 601–612. doi:10.1016/j.eurpolymj.2008.11.017.

[24] A. Dorfmann, R. Ogden, A constitutive model for the mullins effect with permanent set in particle-reinforced rubber, International Journal of Solids and Structures 41 (7) (2004) 1855–1878. doi:10.1016/j.ijsolstr.2003.11.014.

[25] M. Klppel, J. Schramm, A generalized tube model of rubber elasticity and stress softening of filler reinforced elastomer systems, Macromolecular Theory and Simulations 9 (9) (2000) 742–754. doi:10.1002/1521-3919(20001201)9:9<742::aid-mats742>3.0.co;2-4.

[26] S. Wang, S. A. Chester, Experimental characterization and continuum modeling of inelasticity in filled rubber-like materials, International Journal of Solids and Structures 136-137 (2018) 125–136. doi:10.1016/j.ijsolstr.2017.12.010.

[27] A. Lion, A constitutive model for carbon black filled rubber: Experimental investigations and mathematical representation, Continuum Mechanics and Thermodynamics 8 (3) (1996) 153–169. doi:10.1007/bf01181853.

[28] H. Qi, M. Boyce, Stress–strain behavior of thermoplastic polyurethanes, Mechanics of Materials 37 (8) (2005) 817–839. doi:10.1016/j.mechmat.2004.08.001.

[29] L. Guo, Y. Wang, High-rate tensile behavior of silicone rubber at various temperatures, Rubber Chemistry and Technology (In-Press). doi:10.5254/rct.19.81562.

[30] X. Li, T. Bai, Z. Li, L. Liu, Influence of the temperature on the hyper-elastic mechanical behavior of carbon black filled natural rubbers, Mechanics of Materials 95 (2016) 136–145. doi:10.1016/j.mechmat.2016.01.010.

[31] Z. Liao, X. Yao, L. Zhang, M. Hossain, J. Wang, S. Zang, Temperature and strain rate dependent large tensile deformation and tensile failure behavior of transparent polyurethane at intermediate strain rates, International Journal of Impact Engineering 129 (2019) 152–167. doi:10.1016/j.ijimpeng.2019.03.005.

[32] Z. Rigbi, Reinforcement of rubber by carbon black, in: Properties of Polymers, Springer Berlin Heidelberg, 2005, pp. 21–68. doi:10.1007/3-540-10204-3_2.

[33] L. Yan, D. A. Dillard, R. L. West, L. D. Lower, G. V. Gordon, Mullins effect recovery of a nanoparticle-filled polymer, Journal of Polymer Science Part B: Polymer Physics 48 (21) (2010) 2207–2214. doi:10.1002/polb.22102.

[34] S. Wang, S. A. Chester, Modeling thermal recovery of the mullins effect, Mechanics of Materials 126 (2018) 88–98. doi:10.1016/j.mechmat.2018.08.002.

[35] J. Plagge, M. Klueppel, Mullins effect revisited: Relaxation, recovery and high-strain damage, Materials Today Communications 20 (2019) 100588. doi:10.1016/j.mtcomm.2019.100588.